ISSN 1674-1056
http://cpb.iphy.ac.cn
http://iopscience.iop.org/cpb
中国物理 B
Chinese Physics
中国物理 Chinese Physics B

Phase separation and super diffusion of binary mixtures ofactive and passive particles

Yan Wang(王艳), Zhuanglin Shen(谌庄琳), Yiqi Xia(夏益祺), Guoqiang Feng(冯国强), Wende Tian(田文得)
Citation: Chin. Phys. B . 2020, 29(5): 053103 . **doi:** 10.1088/1674-1056/ab81f4
Journal homepage: http://cpb.iphy.ac.cn; http://iopscience.iop.org/cpb

What follows is a list of articles you may be interested in

Control water molecules across carbon-based nanochannels

Xianwen Meng(孟现文), Jiping Huang(黄吉平)
Chin. Phys. B . 2018, 27(1): 013101 . **doi:** 10.1088/1674-1056/27/1/013101

Anisotropic self-diffusion of fluorinated poly(methacrylate) in metal-organic frameworks assessed with molecular dynamics simulation

Tao Lu(鲁桃), Biao Xu(徐彪), Fei-Hong Ye(叶飞宏), Xin-Hui Zhou(周馨慧), Yun-Qing Lu(陆云清), Jin Wang(王瑾)
Chin. Phys. B . 2017, 26(12): 123104 . **doi:** 10.1088/1674-1056/26/12/123104

Effect of grain boundary structures on the behavior of He defects in Ni: An atomistic study

H F Gong(龚恒风), Y Yan(严岩), X S Zhang(张显生), W Lv(吕伟), T Liu(刘彤), Q S Ren(任啟森)
Chin. Phys. B . 2017, 26(9): 093104 . **doi:** 10.1088/1674-1056/26/9/093104

Molecular dynamics simulation of decomposition and thermal conductivity of methane hydrate in porous media

Ping Guo(郭平), Yi-Kun Pan(潘意坤), Long-Long Li(李龙龙), Bin Tang(唐斌)
Chin. Phys. B . 2017, 26(7): 073101 . **doi:** 10.1088/1674-1056/26/7/073101

Phase equilibrium of $Cd_{1-x}Zn_xS$ alloys studied by first-principles calculations and Monte Carlo simulations

Fu-Zhen Zhang(张付珍), Hong-Tao Xue(薛红涛), Fu-Ling Tang(汤富领), Xiao-Kang Li(李小康), Wen-Jiang Lu(路文江), Yu-Dong Feng(冯煜东)
Chin. Phys. B . 2016, 25(1): 013103 . **doi:** 10.1088/1674-1056/25/1/013103

SPECIAL TOPIC — Active matters physics

Phase separation and super diffusion of binary mixtures of active and passive particles*

Yan Wang(王艳)[1,2], Zhuanglin Shen(谌庄琳)[2], Yiqi Xia(夏益祺)[2], Guoqiang Feng(冯国强)[2], and Wende Tian(田文得)[2,3,†]

[1] National Laboratory of Solid State Microstructures and Department of Physics, Collaborative Innovation Center of Advanced Microstructures, Nanjing University, Nanjing 210093, China
[2] Center for Soft Condensed Matter Physics & Interdisciplinary Research, School of Physical Science and Technology, Soochow University, Suzhou 215006, China
[3] Department of Chemical Engineering, Macromolecular Science and Engineering, University of Michigan, Ann Arbor, Michigan 48109, United States

(Received 16 November 2019; revised manuscript received 10 March 2020; accepted manuscript online 23 March 2020)

Computer simulations were performed to study the dense mixtures of passive particles and active particles in two dimensions. Two systems with different kinds of passive particles (e.g., spherical particles and rod-like particles) were considered. At small active forces, the high-density and low-density regions emerge in both systems, indicating a phase separation. At higher active forces, the systems return to a homogeneous state with large fluctuation of particle area in contrast with the thermo-equilibrium state. Structurally, the rod-like particles accumulate loosely due to the shape anisotropy compared with the spherical particles at the high-density region. Moreover, there exists a positive correlation between Voronoi area and velocity of the particles. Additionally, a small number of active particles capably give rise to super-diffusion of passive particles in both systems when the self-propelled force is turned on.

Keywords: phase separation, super diffusion, active particles, binary mixtures

PACS: 31.15.at **DOI:** 10.1088/1674-1056/ab81f4

1. Introduction

Active matter refers to a variety of systems ranging from schools of fish on a macroscale to swarms of bacteria on a microscopic scale.[1] The common feature of these systems is that the constituents locally convert energy into motion. At a high density of constituent units, these systems can be viewed as a living material with the ability to adapt to stimuli, heal itself, like a biological tissue.[2] The far-from-equilibrium feature of these systems leads to rich phenomena such as giant fluctuation,[3–5] phase separation,[6] and super-diffusion.[7–9]

It was shown that active systems consisting of self-propelled particles interacting solely via repulsive interaction phase separate into a solid-like phase and a gas-like phase at very low area fractions in two dimensions.[10] This motility induced phase separation (MIPS) has been observed in many simulations of self-propelled particles[11,12] and also realized experimentally in a system of colloids.[13] However, it is very challenging to reach a high packing fraction in experiments of pure self-propelled particles to investigate the phase-separation behaviors. Most experiments have been carried out with highly diluted suspension of self-propelled particles.[14] Thus, numerical experiments were performed to study the complex phase behavior of dense self-propelled systems.

Recently, the mixtures of self-propelled particles (SPPs) and passive particles or chains in two dimensions have been intensively studied.[15–17] The mixtures provide an additional degree of control for performing specific functions. For example, self-propelled particles lead to the globule–stretch transition of a self-attracting chain due to shear-induced stretching at a low rotational diffusion of SPPs or collision-induced melting at a high rate of SPPs.[18] The mixtures of monodisperse repulsive active Brownian particles and their passive counterparts also display a MIPS behavior, similar to the monodisperse active system, except the existence of enhanced fluctuations and frequent fission and fusion of clusters.[19] The big passive athermal particles display an effective attraction in the bath of small SPPs, which leads to a true phase separation for large size rations and area fraction of SPPs.[17] Recent experiments and simulations also focused on the passive tracers with various shapes such as ellipsoid,[20] chevrons,[21] and wedge[22] in the active suspensions, and found the existence of enhanced diffusion in the translational and rotational degrees. Although there are lots of works on monodisperse SPPs and mixtures of spherical passive particles and SPPs at high area fractions,[15,19,23–25] the mixture of rod-like particles and SPPs has not been investigated so far.[26]

In this paper, we computationally study a binary active mixture of rod-like particles and SPPs with total area frac-

*Project supported by the National Natural Science Foundation of China (Grant Nos. 21674078, 21474074, 21574096, 21774091, and 21374073) and Overseas Research Program of Jiangsu, China (2019).

†Corresponding author. E-mail: tianwende@suda.edu.cn

© 2020 Chinese Physical Society and IOP Publishing Ltd

tion $\varphi_0 = 0.6$, using the active Brownian particle model. Here we focus on the low ratio of SPPs with the area fraction $\varphi_a \sim 0.015$ (i.e., the area fraction of the passive particles is 0.585), which is easy to be realized in colloidal systems.[27] Meanwhile, we also study the mixture of monodisperse SPPs and passive particles with the same fraction and the same ratio of SPPs. We address the following questions. What is the effect of the self-propelled force on the structure and dynamics of the two systems? And what is the structural difference between the two systems? We find both systems exhibit phase separation and super-diffusion as the self-propelled force is turned on, and the phase separation disappears at a large self-propelled force. Structurally, the rod-like particles accumulate loosely compared with the spherical particles at high-density regions due to the shape anisotropy.

The structure of this paper is as follows. We first outline our model and computational methods for both binary-mixture systems. Then, we describe our results and give necessary discussion. Finally, we provide the conclusion and outlook.

2. Model and methods

Our dimer system consists of a binary mixture of N_r rod-like particles (or $N_p = 2N_r$ passive beads for the monomer system) and N_a SPPs moving on a two-dimensional frictional substrate (Fig. 1). Each SPP has its inherent orientation represented by a unit vector, $\boldsymbol{n}_i(\theta_i) = (\cos\theta_i, \sin\theta_i)$, where θ_i is the angle between SPP's orientation and the reference X-axis. This angle is subjected to rotational diffusion, as described by the rotational Brownian equation $\dot{\theta} = \sqrt{2D_r}\xi_\gamma(t)$, where D_r is the rotational diffusivity and ξ_γ is the Gaussian white noise with unit variance.[28]

To mimic the passive rod-like particles, two beads are connected by a stiff harmonic spring via a harmonic potential $U_{\text{bond}} = \frac{1}{2}k(r-r_0)^2$, where $k = 10000k_BT/\sigma^2$ is the spring constant, r is the center-to-center distance between the two bonded beads, and $r_0 = 1.0$ denotes the equilibrium distance. Here, k_BT is used as the energy unit, and σ is the length unit. For the monomer system, the passive particle is similar to the SPPs without inherent orientation.

The motion of each bead with constant mass m is governed by Newton's equation[29]

$$m\ddot{\boldsymbol{r}}_i = \boldsymbol{F}_i^{\text{p}} + \boldsymbol{F}_i^{\text{a}} + \boldsymbol{F}_i^{\text{S}}, \tag{1}$$

where $\boldsymbol{F}_i^{\text{p}}$ is the pairwise interaction force (defined below) on particle i, and $\boldsymbol{F}_i^{\text{a}} = F_a\boldsymbol{n}_i(\theta)$ is the self-propulsion force exerted on the self-propelled particles; for the passive particles, $\boldsymbol{F}_i^{\text{a}} = 0$. $\boldsymbol{F}_i^{\text{S}} = -\gamma_S\boldsymbol{v}_i$ is the Stokes friction acting on particle i.

The pairwise interaction $\boldsymbol{F}_i^{\text{p}}$ of the model is based on the dissipative particle dynamics (DPD) method[30]

$$\boldsymbol{F}_i^{\text{p}} = \sum_{i\neq j}\left(\boldsymbol{f}_{\text{D}}^{ij} + \boldsymbol{f}_{\text{R}}^{ij}\right) - \nabla_i V(r), \tag{2}$$

where $\boldsymbol{f}_{\text{D}}^{ij}$ denotes the purely dissipative force, and $\boldsymbol{f}_{\text{R}}^{ij}$ is the corresponding random force. The dissipative force is given by

$$\boldsymbol{f}_{\text{D}}^{ij} = -\gamma_{\text{dpd}}w^2(r)\left[(\boldsymbol{v}_i - \boldsymbol{v}_j)\cdot\hat{\boldsymbol{e}}^{ij}\right]\hat{\boldsymbol{e}}^{ij}, \tag{3}$$

and the random force is given by

$$\boldsymbol{f}_{\text{R}}^{ij} = \zeta w(r)\alpha^{ij}(\Delta t)^{-\frac{1}{2}}\hat{\boldsymbol{e}}^{ij}. \tag{4}$$

Here, $\hat{\boldsymbol{e}}^{ij} = (\boldsymbol{r}_i - \boldsymbol{r}_i)/r$ is the unit vector directed from particle i to particle j, $w(r) = 1 - r/r_c$ is the weighting function, α^{ij} is a random number, r is the noise strength, and Δt is the simulation timestep. In order to satisfy the fluctuation–dissipation theorem, the relation $\zeta^2 = 2\gamma_{\text{dpd}}k_BT$ is followed.

The pair interaction between any two beads in the system is modeled with a purely repulsive Weeks–Chandler–Andersen (WCA) potential

$$V(r) = 4\varepsilon\left[\left(\frac{\sigma}{r}\right)^{12} - \left(\frac{\sigma}{r}\right)^{6}\right] \tag{5}$$

for distances $r < 2^{1/6}\sigma$, otherwise $V(r) = 0$. Here r is the center-to-center distance between any two particles, and $\varepsilon = 10k_BT$.

All simulations have been performed in a square box of size $100\sigma \times 100\sigma$ with periodic boundary conditions using the home-modified LAMMPS software.[31] The dimer system consists of $N_r = 3700$ rod-like particles and $N_a = 200$ SPPs. The monomer system consists of $N_p = 7400$ passive beads and $N_a = 200$ SPPs, insuring that the area fraction of the active particles is $\varphi_a \sim 0.015$. We use m, σ, and k_BT as the fundamental units for mass, length, and thermal energy, respectively. The simulations parameters are chosen as $m = 1$, $\sigma = 1$, $k_BT = 1$, $\gamma_{\text{dpd}} = 5.0$, and $D_r = 10^{-3}$. We set $\gamma_S = 0.1$ for $F_a \neq 0$. But we technically set $\gamma_S = 0$ when the active force is turned off with the aim of getting enough samples of typical structures. The dimensionless time unit is $\tau = \sqrt{m\sigma^2}/k_BT$. The integration time step is set to $\Delta t = 10^{-3}\tau$ for small self-propelled force and $\Delta t = 5\times10^{-4}\tau$ for large self-propelled force to ensure stable simulation results. In all simulations, the system typically runs up to 10^7 steps.

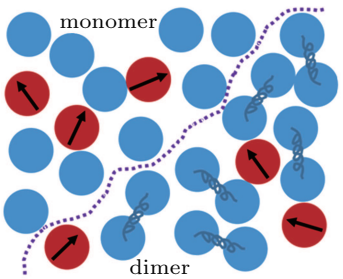


Fig. 1. Schematic of two systems, i.e., a monomer system consisting of monodisperse particles (blue) and self-propelled particles (SPPs) and a dimer system including rod-like particles and SPPs (red). The rod-like particle is composed of two monodisperse spheres connected by a stiff harmonic spring. The arrow indicates the orientation of the SPP which rotates under the thermal fluctuation. The eye-guiding dot line is drawn to separate the two systems.

3. Results and discussion

Figure 2 shows the typical structures of the monomer and dimer systems at self-propelled forces $F_a = 0$, 1, 40. At $F_a = 0$, the system is in the thermodynamic equilibrium, which yields a homogeneous particle distribution. Afterwards the self-propelled force is turned on so that the active particles start performing active motion and colliding with nearby passive particles. Such collisions cause the creation of depleted regions behind the SPPs and the compression of the passive particles. For the monomer system, this is similar to what is observed in the recent experiment.[27] For both systems, the SPPs result in the formation and compression of the clusters of passive particles at $F_a = 1$ (also see the supplemental movies). Thus, the phase separation characterized by the high-density and low-density regions forms. For the monomer system, the passive particles show a crystal-like cluster surrounded by many SPPs at the high-density region. The crystal-like cluster forms and vanishes with the evolution of simulation time. The crystal-like cluster melts from the boundary due to the continual collision with surrounding SPPs, which is in good agreement with a recent numerical simulation.[32] For the dimer system, the degree of crystallization is very weak due to the rod-like shape of the passive particles. The distribution of SPPs is more random than that in the monomer system, in which the SPPs localize at the boundaries of the clusters. At $F_a = 40$, the distribution of particles in both systems becomes homogenous again. The phenomenon not obtained by the experiment and simulation[27] may be due to the low velocity of the colloidal particles. The explanation is as follows: the effective temperature (data not shown) of the system increases with the active force of SPPs due to frequent collisions, the depleted region can be easily filled by the high-velocity passive particles. Besides, the melting of the small clusters is very fast even though they might emerge transiently. This is why the homogenous state with enhanced area variations is observed.

There are three mechanisms of phase separation in binary mixture systems with purely repulsive interaction. One is the depletion-induced phase separation. The depletion effect induces an attractive force between large particles in the mixture because of the unbalanced osmotic pressure exerted on them by the surrounding small particles.[17] Active particles can also induce effective attraction between large passive colloidal particles, known as the active depletion.[33] Under these conditions, the range and strength of the effective attraction are crucially dependent on the shape and size of the passive particle. It was also found that the eccentric active particles can push passive spheres to form a large dense dynamic cluster, and the mixture of the passive spheres and eccentric active particles undergoes a dynamic de-mixing transition due to the entropy-driven depletion.[34] The second one is the diffusivity-induced phase separation in binary mixtures of monodisperse particles. An effective attractive interaction between the low diffusive particles results from the cage-effect by the surrounding high diffusive particles.[35] The third one is the motility-induced phase separation[36] and active–passive segregation.[19] The active–passive mixture shows enhanced fluctuations, with frequent fission and fusion of clusters. The clusters are not homogeneous, but are predominantly active at the periphery and passive in their interior. Our mechanism is similar to the MIPS, which is critically dependent on Péclet number (Pe) of the active particles. Here $Pe \sim \upsilon/\sqrt{D_t D_r}$, where $\upsilon \sim \frac{F_a}{(\gamma_{dpd}+\gamma_S)}$ is the swim velocity of an isolated particle and $D_t = \frac{k_B T}{(\gamma_{dpd}+\gamma_S)}$ is the translational diffusion coefficient. It could be estimated that Pe ranges from ~ 15 to ~ 280 for the separation in our systems.

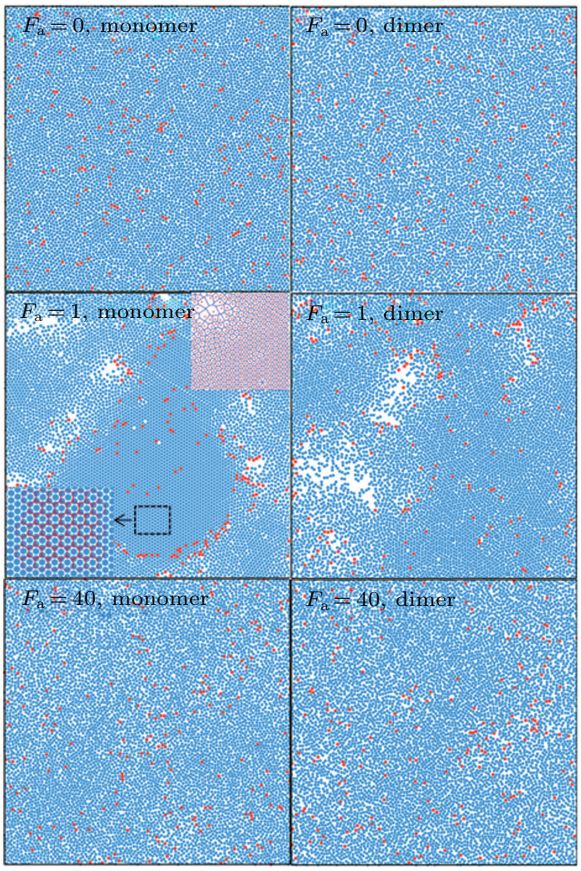


Fig. 2. Snapshots of the monomer and dime systems at various self-propelled forces. SPPs are represented as red disks and passive particles including passive spheres and rod-like particles are represented as blue disks. The inset in the upper-right corner is the corresponding Voronoi cells for part of the monomer system at $F_a = 1$. The Voronoi area is the area of each polygon with blue edge in the inset. The inset in the lower-left corner is the enlarging crystal-like cluster for part of the monomer system at $F_a = 1$.

To qualitatively compare the structures of the two systems with the increase in self-propelled force, we first calculate the Voronoi area, S, of each bead (here we use "bead" to distinguish "particle", because a rod-like particle consists of two beads). Figure 3 shows the deviation of the bead area, $\langle \delta S^2 \rangle = \langle (S - S_0)^2 \rangle$ (here S_0 is equal to the box area over

bead number) as well as the average area, $\langle S \rangle$, of the passive particles and active particles. It can be seen from Fig. 3(a) that, for the homogenous equilibrium state ($F_a = 0$), the deviation is very small (< 0.02). When the active force is turned on, the deviation increases to 0.11, corresponding to the phase separation of the two systems. Then the deviation decreases with the active force of SPPs, implying that the system gradually turns to a homogeneous state. Interestingly, the deviation shows a slight increase with a further increase in active force in both cases. However, the minimal value of $\langle \delta S^2 \rangle$ of the active system is larger than that in the equilibrium state. This implies that the systems with a slightly large fluctuation at the high active force of SPPs are different from the thermo-equilibrium system.

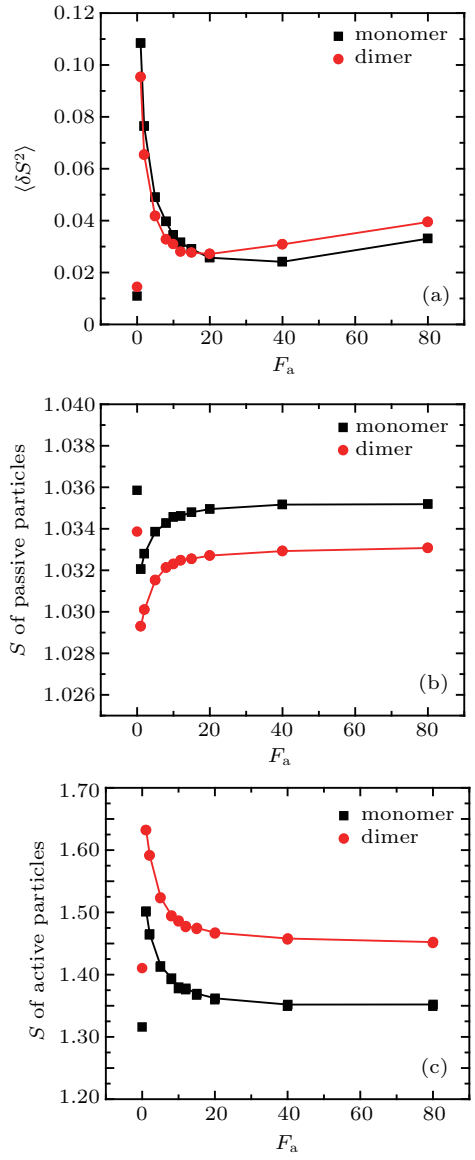


Fig. 3. (a) The deviation of Voronoi area as a function of F_a. The average Voronoi area of (b) passive beads and (c) active particles as a function of F_a for both systems.

The average area of the passive beads increases with the increase in active force, while that of the active particles decreases with the increase in active force (Figs. 3(b) and 3(c)). Both of them plateau to a nearly constant value for high active force. The difference is that the value of $\langle S \rangle$ for the passive beads of the monomer system is larger than that of the dimer system. The discrepancy results from the shape difference of spherical particles and rod-like particles. As expected, the average area of the active particle shows an opposite trend due to the area conservation of the systems.

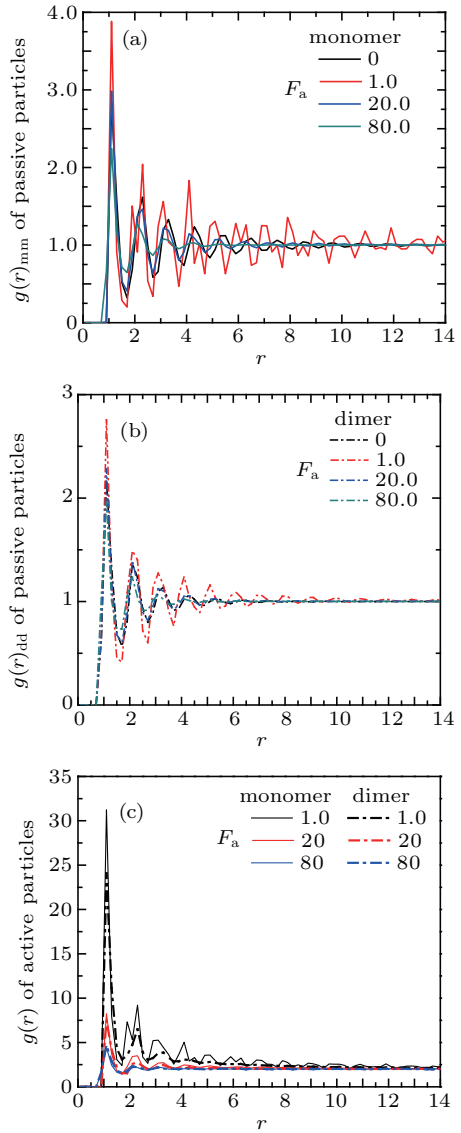


Fig. 4. The PCF of passive particles for (a) the monomer system and (b) the dimer system. (c) The PCF of active particles for both systems at various F_a.

To get the quantitative difference of the structure of the binary mixture, we calculate the pair correlation functions (PCFs), $g(r)$, between the particle pairs. It is a measure of the probability of finding a bead around the reference one. We present the PCFs between passive particles in Fig. 4 for the monomer, $g(r)_{mm}$, and dimer, $g(r)_{dd}$, systems, and $g(r)$ between active particles at the corresponding self-propelled forces. It can be found that there are many peaks of $g(r)_{mm}$ due to the dense mixture we used at the equilibrium state, as shown in Fig. 4(a), indicating a layer-like structure in the sys-

tem. When the active force is turned on, the peaks become higher, especially, the first peak and the appearance of many new peaks at large radial distances, r, relative to the equilibrium case, implying the compression of the passive particles, which is in good agreement with the typical snapshot of Fig. 1. As the active force further increases, the peak drops and disappears at large r (as shown in Fig. 4(a) at $F_a = 20$ and $F_a = 80$). It should be noted that the PCF can not give the information of phase separation. The behavior of PCFs for the dimer system (Fig. 4(b)) is similar to that for the monomer system. The differences are that: 1) the first peak for each F_a shows a little drop because of the spring connection of the two beads of the rod-like particles; 2) the peaks vanish at a moderately shorter distance, indicating a slightly loose packing of rod-like particles compared with that of the monomer system.

To further clarify the difference between the two systems, we also present $g(r)$ of active particles in both systems for various active forces in Fig. 4(c). One can find that the $g(r)$ peaks of active particles for the dimer system at $F_a = 1.0$ are lower than those for the monomer system. Also, the second and third peaks show a slight shift to large r value. This indicates that the layer structure of the active particles in the dimer system is looser than that in the monomer system. At $F_a = 20$ and 80, the behavior of $g(r)$ shows little difference. And the peak is very low compared to that at $F_a = 1.0$. This implies that a homogenous structure reappears.

To study the correlation between velocity and area of the particles, we give the joint probability of velocity and Voronoi area of the active particles in Fig. 5 for the two systems at $F_a = 1.0$, 5.0, 20.0, respectively. Here the velocity is the average velocity of particles per τ. It can be seen that the distribution of the particle area moderately expands with the increase in the self-propelled force. The area of the active particles in the monomer system is between 1.1 and 1.6. While it is between 1.1 and 1.75 in the dimer system. Furthermore, the particle velocity increases with the increase in self-propelled force for both systems. Moreover, the joint probability also shows that the higher the particle's velocity is, the larger the area is, especially, for the case of the small self-propelled force. This indicates that here exists a positive correlation between the Voronoi area and velocity of the particles. Intuitively, the high velocity of SPPs will keep a large depleted region under the same response time (or average velocity) of the passive particles.

To obtain the influence of SPP on the dynamics of the passive particles, we measure the mean square displacements (MSD) of the passive particles, $\langle (r(t))^2 \rangle = \langle (r(t) - r(0))^2 \rangle$, at various F_a for both systems. We also calculate the scaling exponent $\beta(t) = \mathrm{d}[\log(\langle (\Delta r(t))^2 \rangle)]/\mathrm{d}[\log(t)]$ varying with time, as shown in Fig. 6. For normal Brownian diffusion, $\beta(t) = 1$. It can be seen that $\beta(t) = 1$ at $F_a = 0$ for both systems. At $F_a = 1.0$, the passive particles exhibit a super-diffusion behavior at a short time scale, then gradually turn to normal diffusion at a long time scale. As shown in Fig. 6(b), $\beta(t)$ decays quickly from ~ 1.8 to ~ 1.0 with the increase in time. At $F_a = 20$, the passive particles sustain the super-diffusive behavior in the window of our simulation time. The β (t) firstly decreases and then increases with time in our simulation time scale, although the MSD should recover the normal diffusion at a very long time. The similar behavior also exists for the copolymer chain immersed in the bath of SPPs.[37] The mechanism of the nonmonotonic behavior of $\beta(t)$ is not clear, possibly due to the formation and melting of a small cluster of passive particles in the system. This result indicates that a very dilute active particle can result in the super-diffusion of the passive particles.

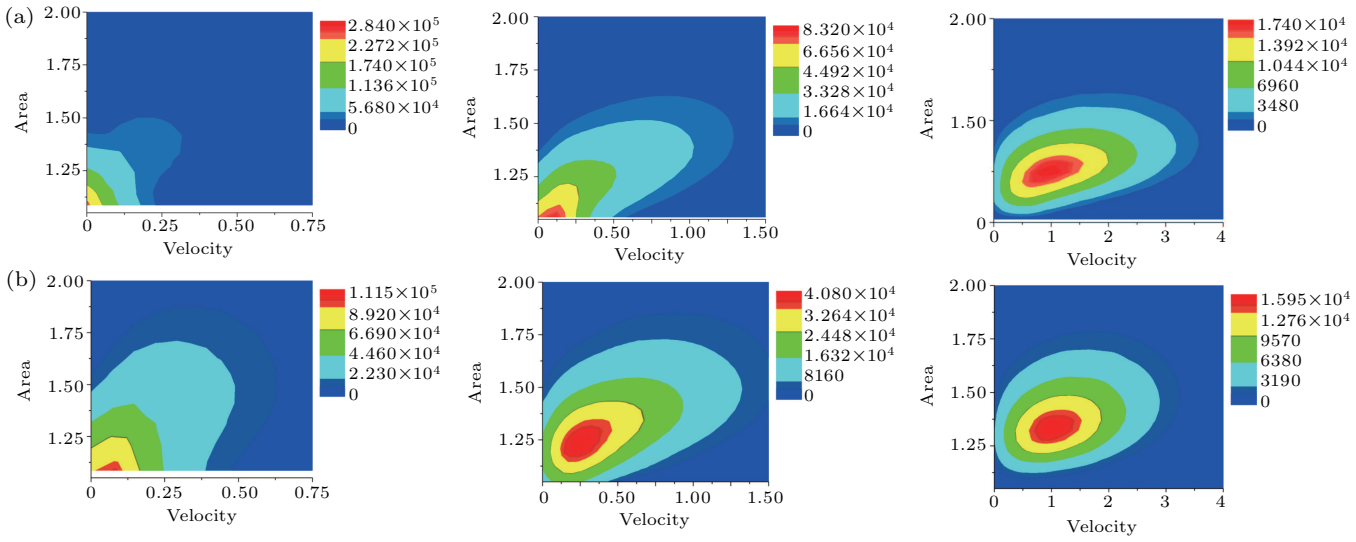


Fig. 5. The joint probability of velocity and Voronoi area of active particle for monomer (a) and dimer (b) systems at $F_a = 1.0$ (left), 5.0 (middle), 20.0 (right).

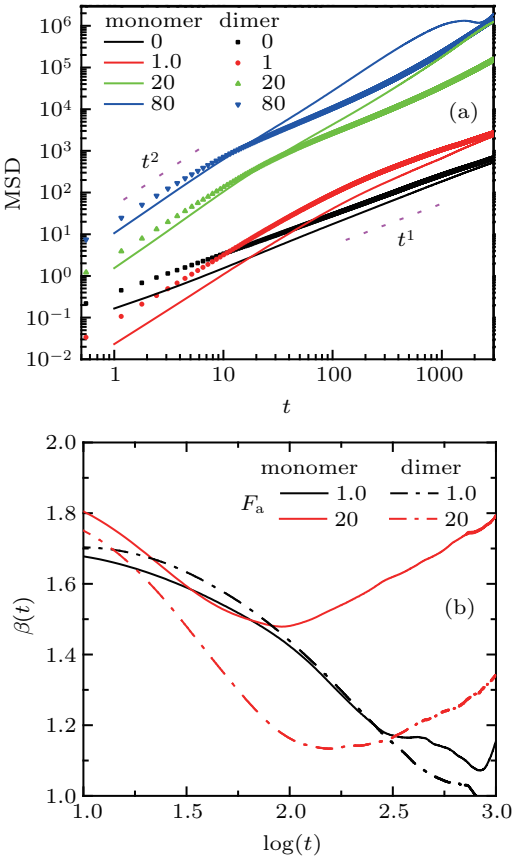


Fig. 6. Log–log plots of (a) the mean square displacement of passive particles for the monomer and dimer systems. The dotted lines show slopes of 2.0 and 1.0. (b) The variations of the scaling exponents $\beta(t)$ for both systems at the indicated self-propelled forces.

4. Conclusion

The study of how SPPs behave in crowded environments resembles realistic situations under which SPPs may be employed, e.g., as drug delivery systems. We performed molecular dynamics simulations with DPD thermostat to study two kinds of binary-mixtures in two dimensions: one is the mixture of passive and self-propelled spheres, the other is the mixture of rod-like particles and self-propelled spheres. Our results show that a very small number of active particles strongly influence the distribution and the dynamics of the dense mixtures. We find that, at a small active force, the high-density and low-density regions appear in both systems, indicating an emergence of phase separation. Then it vanishes at higher active forces due to the velocity improvement induced by frequent collision. Structurally, the rod-like particles accumulate loosely due to the shape anisotropy, compared with the spherical particles at the high-density region. In addition, we find the existence of positive correlation between Voronoi area and velocity of particles in both systems. Moreover, the passive particles show a super-diffusive behavior when the self-propelled force is turned on in spite of the low fraction of the active particles.

Here, we focus only on the dense systems with a low fraction of SPPs. In the future, the fraction effect of SPPs will be studied and the phase diagram might be given for the rod-like particle system.[38] Besides, the length of the rod-like particles is another interesting parameter that should be studied in further work.[39]

References

[1] Popkin G 2016 *Nature* **529** 16
[2] Bernheim-Groswasser A, Gov N S, Safran S A and Tzlil S 2018 *Adv. Mater.* **30** 1707028
[3] Shi X and Ma Y 2013 *Nat. Commun.* **4** 3013
[4] Zhang H P, Be'er A, Florin E L and Swinney H L 2010 *Proc. Natl. Acad. Sci. USA* **107** 13626
[5] Zhang R, Ren C, Feng J and Ma Y 2019 *Sci. Chin. Phys. Mech. Astron.* **62** 117012
[6] Shi X Q and Ma Y Q 2010 *Proc. Natl. Acad. Sci. USA* **107** 11709
[7] Tian W D , Gu Y, Guo Y K and Chen K 2017 *Chin. Phys. B* **26** 100502
[8] Li H, Wang C, Tian W, Ma Y, Xu C, Zheng N and Chen K 2017 *Soft Matter* **13** 8031
[9] Li H, Zhang B, Li J, Tian W and Chen K 2015 *J. Chem. Phys.* **143** 224903
[10] Fily Y and Marchetti M C 2012 *Phys. Rev. Lett.* **108** 235702
[11] Shan W, Zhang F, Tian W and Chen K 2019 *Soft Matter* **15** 4761
[12] Agudo-Canalejo J and Golestanian R 2019 *Phys. Rev. Lett.* **123** 018101
[13] Dietrich K, Volpe G, Sulaiman M N, Renggli D, Buttinoni I and Isa L 2018 *Phys. Rev. Lett.* **120** 268004
[14] Palacci J, Sacanna S, Steinberg A P, Pine D J and Chaikin P M 2013 *Science* **339** 936
[15] Kolb T and Klotsa D 2020 *Soft Matter* **16** 1967
[16] Nilsson S and Volpe G 2017 *New J. Phys.* **19** 115008
[17] Dolai P, Simha A and Mishra S 2018 *Soft Matter* **14** 6137
[18] Xia Y, Tian W, Chen K and Ma Y 2019 *Phys. Chem. Chem. Phys.* **21** 4487
[19] Stenhammar J, Wittkowski R, Marenduzzo D and Cates M E 2015 *Phys. Rev. Lett.* **114** 018301
[20] Peng Y, Lai L, Tai Y S , Zhang K, Xu X and Cheng X 2016 *Phys. Rev. Lett.* **116** 068303
[21] Restrepo Pérez L, Soler L, Martínez-Cisneros C S, Sánchez S and Schmidt O G 2014 *Lab Chip* **14** 1515
[22] Kaiser A, Sokolov A, Aranson I S and Löwen H 2015 *Eur. Phys. J. Spec. Top.* **224** 1275
[23] Hinz D F, Panchenko A, Kim T Y and Fried E 2014 *Soft Matter* **10** 9082
[24] Belan S and Kardar M 2019 *J. Chem. Phys.* **150** 064907
[25] Wysocki A, Winkler R G and Gompper G 2016 *New J. Phys.* **18** 123030
[26] Mandal R, Bhuyan P J, Chaudhuri P, Rao M and Dasgupta C 2017 *Phys. Rev. E* **96** 042605
[27] Kümmel F, Shabestari P, Lozano C, Volpe G and Bechinger C 2015 *Soft Matter* **11** 6187
[28] Yang Q, Fan Q, Shen Z, Xia Y, Tian W and Chen K 2018 *J. Chem. Phys.* **148** 214904
[29] Lobaskin V and Romenskyy M 2013 *Phys. Rev. E* **87** 052135
[30] Hinz D F, Panchenko A, Kim T Y and Fried E 2015 *Comput. Phys. Commun.* **196** 45
[31] Plimpton S 1995 *J. Comput. Phys.* **117** 1
[32] Ni R, Stuart M A C and Dijkstra M 2013 *Nat. Commun.* **4** 2704
[33] Ni R, Cohen Stuart M A and Bolhuis P G 2015 *Phys. Rev. Lett.* **114** 018302
[34] Ma Z, Lei Q L and Ni R 2017 *Soft Matter* **13** 8940
[35] Weber S N, Weber C A and Frey E 2016 *Phys. Rev. Lett.* **116** 058301
[36] Mandal S, Liebchen B and Löwen H 2019 *Phys. Rev. Lett.* **123** 228001
[37] Xia Y, Shen Z, Tian W and Chen K 2019 *J. Chem. Phys.* **150** 154903
[38] Bakker H E, Dussi S, Droste B L, Besseling T H, Kennedy C L, Wiegant E I, Liu B, Imhof A, Dijkstra M and van Blaaderen A 2016 *Soft Matter* **12** 9238
[39] Rodríguez-Liñán G M, Nahmad-Molinari Y and Pérez-Ángel G 2016 *PLoS One* **11** e0156153